Beyond the Maxwell limit: Thermal conduction in nanofluids with percolating fluid structures

Jacob Eapen*
Theoretical Division (T-12), Los Alamos National Laboratory, Los Alamos, New Mexico 87545, USA

Ju Li
Department of Materials Science and Engineering, Ohio State University, Columbus, Ohio 43210, USA

Sidney Yip
Department of Nuclear Science and Engineering, Massachusetts Institute of Technology, Cambridge, Massachusetts 02139, USA
(Received 6 August 2007; published 17 December 2007)

In a well-dispersed nanofluid with strong cluster-fluid attraction, thermal conduction paths can arise through percolating amorphouslike interfacial structures. This results in a thermal conductivity enhancement beyond the Maxwell limit of 3ϕ, with ϕ being the nanoparticle volume fraction. Our findings from nonequilibrium molecular dynamics simulations, which are amenable to experimental verification, can provide a theoretical basis for the development of future nanofluids.

DOI: 10.1103/PhysRevE.76.062501 PACS number(s): 65.80.+n, 68.08.−p, 68.05.Cf, 81.05.Zx

Mean-field theories are largely successful for characterizing the thermal conduction behavior in nanofluids [1–3]. In particular, the thermal conductivity of most nanofluids is well characterized by the dilute limit of 3ϕ from the classical Maxwell's theory for well-dispersed, spherical nanoparticles, with ϕ denoting the nanoparticle volume fraction [1]. Several recent experiments, however, show conflicting behavior such as increasing thermal conductivity with decreasing nanoparticle size [4], saturation at higher volume fractions [5], an apparent lack of correlation to the intrinsic thermal conductivity of the nanoparticles [5,6], and a relatively large thermal conductivity enhancement at low volume fractions (18–25 % with $\phi \leq 1\%$) [5,7].

From a theoretical perspective, a key challenge is to understand the possible mechanisms that can increase the thermal conductivity beyond the 3ϕ Maxwell limit. The postulated Brownian-motion or microconvection mechanisms [8] have been shown to be untenable through experimental [9] and theoretical studies [10]. Two recent studies, a modification of the mean-field theory [11] and our equilibrium (Green-Kubo) molecular dynamics simulation of small clusters [12], open up interesting theoretical possibilities. In the first, the thermal conductivity is shown to increase by percolation through a chainlike agglomeration of the nanoparticles [11,13]. In the second, we find an enhancement in the thermal conductivity originating from the correlation in the potential energy flux [12].

In this Brief Report, we demonstrate using nonequilibrium molecular dynamics simulations (NEMD) that the thermal conductivity of a well-dispersed nanofluid is enhanced beyond the 3ϕ Maxwell limit through a percolating amorphouslike *fluid* structure at the cluster interface. These interconnected paths emerge only when the cluster-fluid interaction is strong; for weak cross interaction the enhancement is only slightly higher than the 3ϕ limit. The attendant changes in interfacial structure are accessible by experimental techniques such as neutron scattering. Our findings suggest a theoretical basis for a systematic development of future nanofluids.

We consider a nanofluid system where solid clusters are dispersed uniformly in a Lennard-Jones (LJ) fluid. The cluster atoms, in addition to experiencing a LJ potential, are held together by a finitely extensible nonlinear elastic (FENE) potential given by $-A\varepsilon \ln[1-(r/B\sigma)^2]$, where ε and σ are the reference values for energy and length, and A and B are two constants, which take the values of 5.625 and 4.95, respectively, in the simulations. The fluid-fluid and solid-fluid (SF) interactions are modeled by LJ interactions with the parameters (ε,σ) and $(\varepsilon_{SF},\sigma)$, respectively. The LJ potential for solid-solid interaction is also given by (ε,σ). The coupling between the solid and fluid atoms is measured through the attractive potential well depth ε_{SF} relative to that between two fluid atoms ε. Reduced units based on m, ε, and σ are used throughout in this study. Our simulations are carried out at a constant temperature of 1.0 and a volume corresponding to zero pressure. At this state point, the radial distribution function (*rdf*) indicates that the base fluid has a structure corresponding to that of a liquid. The cluster configuration consists of ten solid clusters of ten atoms each in a host fluid of 1948 atoms leading to a number fraction of 4.88%. The volume fraction is calculated as $\pi n\rho d^3/6\nu$, where n is the solid atom number fraction, ρ is the number density, and d and $\nu \approx 0.7405$ are the nearest-neighbor distance and the packing fraction in a face-centered cubic lattice, respectively. The ratio d^3/ν assigns the void space between the solid atoms to the cluster volume.

NEMD simulation is conducted through the imposed-flux method [14] where a temperature profile develops with the imposition of a known heat flux. This method is compatible with periodic boundary conditions, conserves both energy and momentum, and experiences only limited perturbation effects. The simulation box is divided into slabs perpendicular to a chosen direction, say, z, with the edge slabs denoted as "cold" and the center slab as "hot." Velocity exchanges are made between atoms of these slabs such that the hottest

*eapen@lanl.gov

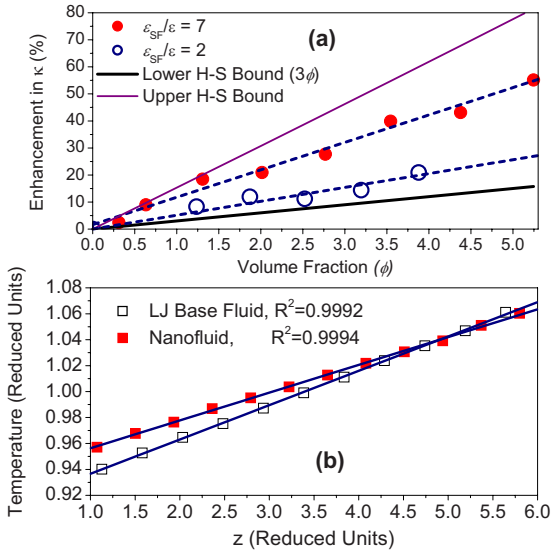

FIG. 1. (Color online) (a) Enhancement in κ for $\varepsilon_{SF}/\varepsilon=7$ and $\varepsilon_{SF}/\varepsilon=2$ at $T=1$ and $P=0$, and the Hashin-Shtrikman (H-S) bounds. (b) Temperature profiles with $\varepsilon_{SF}/\varepsilon=7$ for $\phi=3.5\%$. R^2 denotes the multiple correlation coefficient.

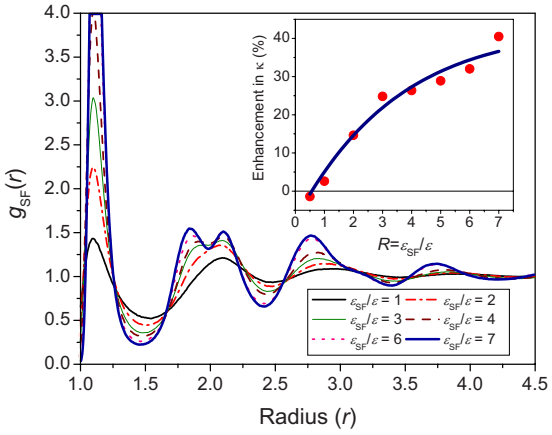

FIG. 2. (Color online) The cross radial distribution function $g_{SF}(r)$ for several values of $\varepsilon_{SF}/\varepsilon$ with $n=100/2048$. The inset shows the increase in the thermal conductivity with $\varepsilon_{SF}/\varepsilon$.

atom in the cold slab is exchanged with the coldest atom in the hot slab. At steady state, a linear temperature profile develops, which is symmetric about the hot slab. The heat flux is computed exactly with the known values of the velocities that are exchanged [14]. The equilibration is done for 100 000 iterations and temperature in each slab is averaged for another 150 000 iterations without the use of a thermostat or barostat. Further averaging over 10–12 initial conditions is needed to average out the statistical variations of the clusters and to generate an acceptable linearity in the temperature profile (measured by the multiple correlation coefficient, $R^2 \geq 0.999$). No significant size dependency has been observed in the simulation results. The thermal conductivity is evaluated from the Fourier's law $\kappa=-\langle \mathbf{J}_q \rangle_z/(dT/dz)$, where $\mathbf{J}_q$ and dT/dz are the heat flux and temperature gradient, respectively.

For the host fluid (without the nanoclusters) we obtain a thermal conductivity (κ_f) of 4.0, which compares well with a Green-Kubo evaluation of 4.1 in reduced units. For a solid atom lattice, having a potential energy (per atom) that is similar to that of the cluster atoms in the nanofluid, a linear response (Green-Kubo) evaluation of the thermal conductivity gives a value of 93 in reduced units. With the parameters of Xe, the thermal conductivity of the fluid and the solid clusters are 0.043 W/m K and 1.00 W/m K, respectively, leading to a ratio $\kappa_p/\kappa_f \sim 23$.

In Fig. 1(a) we show that the κ enhancements with the weak ($\varepsilon_{SF}/\varepsilon=2$) as well as the strong cluster-fluid attraction ($\varepsilon_{SF}/\varepsilon=7$) increase linearly with ϕ. The thermal conductivities are evaluated from well-converged temperature profiles as shown in Fig. 1(b). For the strong cross attraction, κ increases with a much larger slope than that of the weak cross attraction, resulting in an enhancement of 55% at a volume fraction of 5.2%. The simulation data, however, are bounded by the formal limits of Hashin-Shtrikman (H-S) mean-field theory [15] wherein the lower limit is identically equivalent to the Maxwell expression for $\kappa_p > \kappa_f$, where κ_p and κ_f are the nanocluster and fluid thermal conductivities. The H-S expression is given by

$$\kappa_f\left(1+\frac{3\phi[\kappa]}{3\kappa_f+(1-\phi)[\kappa]}\right) \leq \kappa \leq \left(1-\frac{3(1-\phi)[\kappa]}{3\kappa_p-\phi[\kappa]}\right)\kappa_p, \tag{1}$$

where $[\kappa]$ is defined as $\kappa_p-\kappa_f$.

For the weaker cross attraction, the enhancements are only slightly larger than the lower H-S bound (Maxwell 3ϕ limit) while for the stronger cross attraction, they are closer to the upper H-S bound. The H-S theory does not give the actual mechanism of thermal conductivity enhancement but sets the most restrictive bounds on the basis of knowing only the volume fraction. Physically, the upper H-S bound corresponds to a nanocluster matrix with spherical inclusions of fluid regions, and the lower H-S bound is for the reverse situation. The upper bound, therefore, is skewed toward a parallel conduction mode between the nanoclusters and fluid atoms, whereas the lower bound favors a series mode. So it is evident that the strong cross attraction introduces conduction paths that are parallel and since the clusters are well dispersed, they are possible only through the mediation of the fluid atoms. We will now explain this behavior by analyzing the interfacial fluid structure.

In Fig. 2, we show the cross radial distribution function $g_{SF}(r)$ for several values of $\varepsilon_{SF}/\varepsilon$ at a volume fraction of 3.5%. For $\varepsilon_{SF}/\varepsilon=2$, the cross radial distribution function, which is the probability of finding a fluid atom at a certain radial location given that a solid atom is at the origin, has the characteristics resembling that of a fluid. As $\varepsilon_{SF}/\varepsilon$ further increases, the fluid atoms in the vicinity of the clusters get more strongly attracted toward the clusters and move inward, as can be seen from the sharpening of the first peak and the emergence of the third peak. Remarkably, the second peak flattens and splits into two, which is a characteristic signature of an amorphouslike transition. The fluid-fluid radial distribution function, on the other hand, is only marginally af-

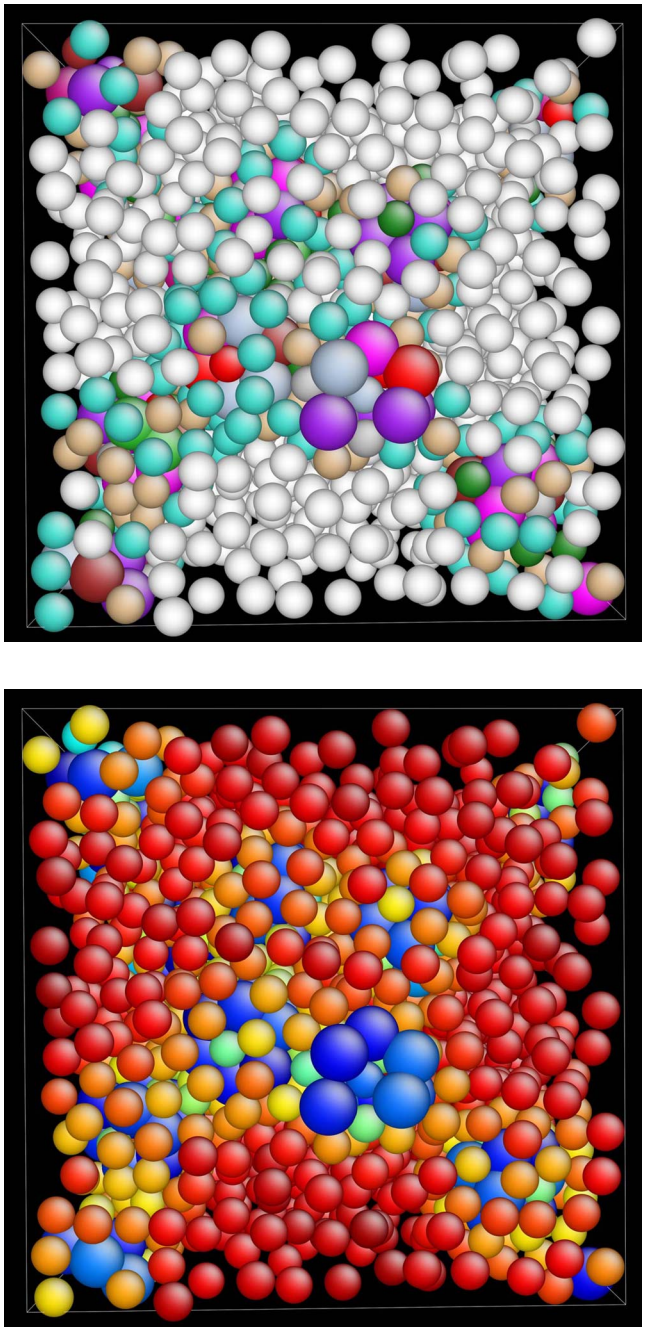

FIG. 3. (Color online) (Top) Coordination number (CN) and potential energy (bottom) maps with $\varepsilon_{SF}/\varepsilon=7$ and $\phi=3.5\%$. Magenta (deep blue) and white (red) in the CN (potential) energy maps denote the (ten) clusters and fluid atoms, respectively. The intermediate colors represent the percolating conduction paths.

fected by the higher values of $\varepsilon_{SF}/\varepsilon$ (not shown). It is thus clear that the fluid atoms pack themselves in a random close pack arrangement only near the vicinity of the solid clusters. Inset (a) shows the enhancement in the thermal conductivity, which increases with $\varepsilon_{SF}/\varepsilon$. Interestingly, a change of slope can be detected beyond $\varepsilon_{SF}/\varepsilon=3$, which is commensurate with a more modest change in the structure of the interfacial fluid atoms.

Thus, a relatively strong cluster-fluid attraction ($\varepsilon_{SF}/\varepsilon \geq 2$) can introduce an amorphouslike fluid structure around the nanoclusters. The mean separation between the clusters is $O(D)$ as given by the dilute limit $D_s=[(\pi/6\phi)^{1/3}-1]D$, where D is the cluster diameter, and D_s the separation distance. This shows that the interface around the clusters forms a percolating network of amorphouslike structure. The coordination number map in Fig. 3 (top), colored by the number of nearest neighbors, shows this percolating interfacial fluid structure. The higher density of fluid atoms along this structure allows a network of excess potential energies as shown in Fig. 3 (bottom), which are instrumental in additional thermal conduction paths either through a potential energy exchange mechanism or a phononlike collision mechanism [12]. The networked paths now favor a parallel mode of conduction and the observed enhancements in the thermal conductivity are closer to the upper H-S bound as observed in Fig. 1.

An alternate approach for analyzing the enhancement beyond the Maxwell limit is through the concept of a negative interfacial thermal (Kapitza) resistance, or equivalently, a negative Kapitza length. The original Maxwell expression [lower bound in Eq. (1)] does not include the interfacial resistance even though this is easily done by substituting $\kappa_f \rightarrow \kappa_f+\alpha\kappa_p$ [in the bracketed terms of Eq. (1)], where $\alpha=2R_b\kappa_f/D$ and R_b is the interfacial thermal resistance [16]. For $\varepsilon_{SF}/\varepsilon<1$ (see the inset of Fig. 2), R_b is positive as inferred from the decrease in the effective thermal conductivity. A positive R_b also corresponds to a positive Kapitza length defined as the ratio of the *extrapolated* temperature drop at the cluster interface to the gradient of the bulk temperature [17,18]. When $\varepsilon_{SF}/\varepsilon$ approaches 1.5, the enhancement is consistent with a Maxwell prediction indicating a negligible R_b. For $\varepsilon_{SF}/\varepsilon$ larger than the critical value of 1.5 (approximately), the Kapitza length turns from positive to negative as a result of the proliferation of interfaces that leads to an increase in the effective thermal conductivity. Physically, a negative Kapitza length indicates an interfacial thermal gradient that is lower than that of the bulk region and vice versa. In contrast, the earlier NEMD investigations on nanofluids, which showed negligible or negative enhancements [10,19], had a positive Kapitza length because of a weak solid-fluid interaction.

In conclusion, we observe that a strong cross attraction between the clusters and fluid atoms in a nanofluid can induce a percolating network of thermal conduction paths mediated by the interfacial fluid atoms. As a result, the thermal conductivity can be enhanced beyond the commonly observed 3ϕ Maxwell limit. Our findings suggest a theoretical basis for a systematic development of future nanofluids with very small nanoclusters.

J.E. acknowledges an interesting discussion with J.-L. Barrat. The work of J.E. and S.Y. is supported by the National Science Foundation under Grant No. 0205411. The work of J.L. is supported by DOE Grant No. DE-FG02-06ER46330.

[1] P. Keblinski, J. A. Eastman, and D. G. Cahill, Mater. Today **8**, 36 (2005).
[2] D. C. Venerus *et al.*, J. Appl. Phys. **100**, 094310 (2006).
[3] R. Rusconi, E. Rodari, and R. Piazza, Appl. Phys. Lett. **89**, 261916 (2006).
[4] S. H. Kim, S. R. Choi, and D. Kim, J. Heat Transfer **129**, 298 (2007).
[5] H. Zhu *et al.*, Appl. Phys. Lett. **89**, 023123 (2006).
[6] T. K. Hong, H. S. Yang, and C. J. Choi, J. Appl. Phys. **97**, 064311 (2005).
[7] H. T. Zhu *et al.*, J. Phys. Chem. C **111**, 1646 (2007).
[8] R. Prasher, P. Bhattacharya, and P. E. Phelan, Phys. Rev. Lett. **94**, 025901 (2005).
[9] J. Eapen *et al.*, Phys. Rev. Lett. **99**, 095901 (2007).
[10] W. Evans, J. Fish, and P. Keblinski, Appl. Phys. Lett. **88**, 093116 (2006).
[11] R. Prasher *et al.*, Appl. Phys. Lett. **89**, 143119 (2006).
[12] J. Eapen, J. Li, and S. Yip, Phys. Rev. Lett. **98**, 028302 (2007).
[13] M. Vladkov and J.-L. Barrat, e-print arXiv:cond-mat/0612249v1, J. Comput. Theor. Nanosci. (to be published).
[14] F. Müller-Plathe, J. Chem. Phys. **106**, 6082 (1997).
[15] Z. Hashin and S. Shtrikman, J. Appl. Phys. **33**, 3125 (1962).
[16] C.-W. Nan *et al.*, J. Appl. Phys. **81**, 6692 (1997).
[17] J.-L. Barrat and F. Chiaruttini, Mol. Phys. **101**, 1605 (2003).
[18] R. Kharea, P. Keblinski, and A. Yethiraj, Int. J. Heat Mass Transfer **49**, 3401 (2006).
[19] M. Vladkov and J.-L. Barrat, Nano Lett. **6**, 1224 (2006).